

**LASER INTERFEROMETER GRAVITATIONAL WAVE OBSERVATORY**  
– LIGO –  
CALIFORNIA INSTITUTE OF TECHNOLOGY  
MASSACHUSETTS INSTITUTE OF TECHNOLOGY

<b>Document Type</b>	<b>LIGO-T010162-00-R</b>	<b>10/15/01</b>
<b>Characterization and Testing of the Optical Properties of the LIGO 40m Lab Pre-Stabilized Laser</b>		
Timofei Piatenko, Alan Weinstein, Dennis Ugolini		

*Distribution of this draft:*

This is an internal working note  
Of the LIGO Project

California Institute of Technology  
LIGO Project – MS 51-33  
Pasadena, CA 91125  
Phone (626)395-2129  
Fax (626)304-9834  
E-mail: [info@ligo.caltech.edu](mailto:info@ligo.caltech.edu)

Massachusetts Institute of Technology  
LIGO Project – MS 20B-145  
Cambridge, MA 01239  
Phone (617)253-4824  
Fax (617)253-7014  
E-mail: [info@ligo.mit.edu](mailto:info@ligo.mit.edu)

WWW: <http://www.ligo.caltech.edu>

Characterization and Testing of the Optical  
Properties of the LIGO 40-meter Lab Pre-Stabilized  
Laser

Timofei Piatenko

Mentors: Alan J. Weinstein and Dennis Ugolini

September 10, 2001

## Abstract

The Pre-Stabilized Laser (PSL) is essential to the LIGO detectors, where precision levels of  $10^{-21}$  on gravitational strain have to be achieved, corresponding to extremely stable operation and low frequency, intensity, and pointing noise of the PSL. The beam has to precisely follow the desired path and transverse profile on the optical table to ensure that elements, such as the reference cavity, perform their tasks properly. My project consists of understanding, characterizing, and testing the optical layout of the PSL.

I have learned the basics of Gaussian optics, which governs laser beam propagation, paying special attention to the concepts of *mode matching* and *mismatch*. I have implemented a set of Matlab routines for calculating the beam path and transverse profile, creating a complete graphical representation, and manipulating the layout to ensure optimal placement of optical elements.

The results of my calculations have uncovered at least one mistake in the layout, which has been promptly corrected, greatly improving the performance of the pre-mode cleaner. The rest of the layout needs verification and optimization. Once the layout is corrected as necessary, short and long-term stability in frequency and intensity has to be studied in detail to fully characterize the performance of the PSL.

# Contents

<b>1</b>	<b>Introduction</b>	<b>4</b>
1.1	Background . . . . .	4
1.2	What is a Gravitational Wave? . . . . .	5
1.3	What is LIGO? . . . . .	5
<b>2</b>	<b>Importance of the PSL</b>	<b>7</b>
2.1	Using the Phase Shift . . . . .	7
2.2	Use of High Power . . . . .	7
<b>3</b>	<b>PSL Operation</b>	<b>8</b>
3.1	Gaussian Beams . . . . .	8
3.2	Guoy Phase Shift . . . . .	10
3.3	Mode Matching . . . . .	10
3.4	Mode Mismatch . . . . .	11
3.5	MOPA Laser . . . . .	11
3.6	Frequency Reference Cavity . . . . .	13
3.7	Pre-Mode Cleaner . . . . .	13
<b>4</b>	<b>Simulating the Beam</b>	<b>14</b>
<b>5</b>	<b>Beam Measurements</b>	<b>14</b>
5.1	Transmission . . . . .	14
5.2	Visibility . . . . .	18
5.3	Transverse Profile . . . . .	18
5.4	Beam Scan . . . . .	18
<b>6</b>	<b>Results</b>	<b>20</b>
6.1	Optical Table . . . . .	20

6.2	Focal Length Measurements . . . . .	21
6.3	Quad Photodiodes . . . . .	22
6.4	Final Measurements . . . . .	22
6.4.1	Transmission . . . . .	22
6.4.2	Visibility and Beam Scan Profile . . . . .	23
6.4.3	Conclusion . . . . .	23
<b>7</b>	<b>Acknowledgments</b>	<b>24</b>

# 1 Introduction

## 1.1 Background

The search for gravitational waves dates back to the beginning of the 20th century, when Einstein's theory of General Relativity forever changed the way physicists view gravity. According to Einstein, gravitational forces result from curvature in four-dimensional space-time. Since all objects move along geodesics in space-time, gravitational forces manifest themselves by altering the four-dimensional surfaces to which the objects are confined.

Einstein also predicted that, similarly to the way an accelerating charge produces electro-magnetic radiation, oscillating gravitational charges (massive bodies) should produce gravitational waves, carriers of gravitational fields. However, Einstein himself doubted that such waves could ever be detected, given their extremely low magnitude. However, as time went by and technology advanced, hopes of detecting gravitational waves heightened.

In 1969, Joseph Weber announced that his detector registered a meaningful signal, sending a shock-wave throughout the scientific community. Although Weber's discovery was never generally accepted by other physicists, it initiated a greater effort to construct highly sensitive detectors, with the LIGO project being one of the direct results.

The importance of LIGO is that it is one of the few experiments aimed at testing the General Relativity theory, which allows for very few experimental techniques. Unlike Maxwell's theory of electromagnetism, gravitational theory cannot be tested by creating an artificial, fully controlled setup on earth because of the extremely small amplitude of gravitational fields compared, for instance, with electro-magnetic radiation. Gravitational wave experiments are confined to looking at astrophysical phenomena.

## 1.2 What is a Gravitational Wave?

According to Einstein's Special Theory of Relativity, the *space-time* interval invariant under Lorentz transformations is given by

$$ds^2 = -c^2 dt^2 + dx^2 + dy^2 + dz^2. \quad (1)$$

or using the matrix notation with Minkowski metric  $\begin{pmatrix} -1 & 0 & 0 & 0 \\ 0 & 1 & 0 & 0 \\ 0 & 0 & 1 & 0 \\ 0 & 0 & 0 & 1 \end{pmatrix}$  it becomes

$$ds^2 = \eta_{\mu\nu} dx^\mu dx^\nu. \quad (2)$$

In General Relativity, a perturbation is introduced to the Minkowski metric in the form of  $\begin{pmatrix} 0 & 0 & 0 & 0 \\ 0 & a & b & 0 \\ 0 & b & -a & 0 \\ 0 & 0 & 0 & 0 \end{pmatrix}$  so that the full metric is now

$$g_{\mu\nu} = \eta_{\mu\nu} + h_{\mu\nu}. \quad (3)$$

The perturbation  $h$ , called *gravitational strain*, satisfies the wave equation (in a certain gauge), and thus can be responsible for a gravitational wave propagating through space-time, changing its geometry. The effects of this wave can be observed as change in length of a particular object in rest in our frame.

## 1.3 What is LIGO?

LIGO (Laser Interferometer Gravitational-Wave Observatory) is the joint MIT-Caltech gravitational wave detector project. There are two LIGO sites, one at Hanford, Washington, the other at Livingston, Louisiana, each consisting of two long (4 km) arms perpendicular to each other. The arms house large vacuum chambers with test masses suspended at each end. A high-power (10 Watt) laser is deployed to monitor the distances between the test masses. The apparatus is set up in the form of a Michelson interferometer (see Figure 2) with folded Fabry-Perot cavities in the two arms, where the laser beam resonates. Any relative displacement of the test masses is detected by observing the output beams, as they interfere upon their recombination.

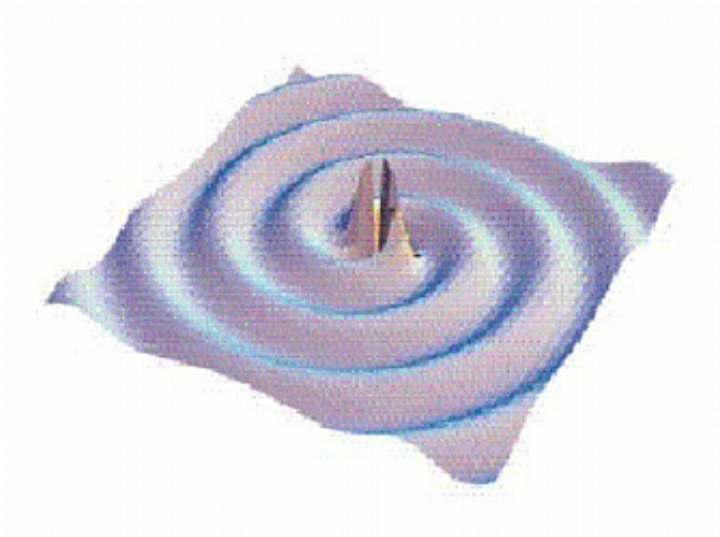


Figure 1: An artist's conception of gravitational waves generated by the inspiral of a compact stellar binary system.

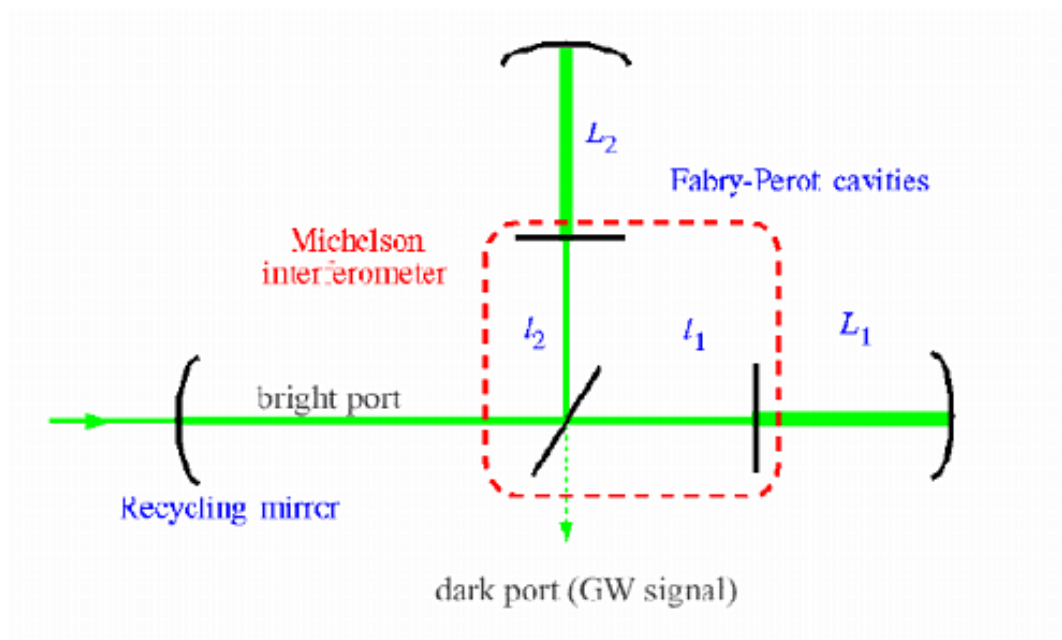


Figure 2: Basic LIGO interferometer layout.



## 2 Importance of the PSL

### 2.1 Using the Phase Shift

In order to measure displacements between the test masses, a laser beam is split into two parts, each going off into its respective arm, where it resonates in the Fabry-Perot cavity. The beams from the two arms are then recombined, and their interference pattern studied. Rather than creating the well-known “fringes” pattern, the beam fronts are made parallel to each other. Thus, the measure of interference comes from observing the resulting power in the recombined output beam. If the two arms are of lengths that differ by  $\Delta L$ , such that  $k\Delta L = \frac{\pi}{2}$ , the beams will come in exactly out-of-phase, and the power will be at its minimum (ideally zero). However, an incident gravitational wave would alter the lengths of the arms (adding  $\delta L$  to one arm and subtracting the same  $\delta L$  from the other), thus causing the two beams to arrive in such a way that they are no longer perfectly out-of-phase, increasing the power in the resulting beam.

The idea is to turn the interferometer into an *active null instrument*, meaning that it is forced to operate in the same regime through the use of feedback loops. The laser light is kept in resonance inside the cavities, even if the lengths are altered. Thus, if the two cavities differ in length, the beams resonating inside will have different frequencies. In the LIGO setup, the laser light phases are initially shifted in the two cavities such that the resulting recombined beam produces a *dark fringe*, but any alteration of the cavity lengths due to gravitational waves or fluctuations in the test mass positions will change this *null state*.

### 2.2 Use of High Power

Since we use the output power as a measure of interference between the two beams resonating in the two arms, we want to be able to measure this quantity as precisely as possible. However, there are some fundamental limitations to how precise we can get.

The *photon shot noise*, defined as

$$h_{shot}(f) = \frac{1}{L} \sqrt{\frac{\hbar c \lambda}{2\pi P_{in} T(f)}}, \quad (4)$$

where  $L$  is the length of the detector,  $\lambda$  is the wavelength of laser light,  $c$ , as usual, the speed of light, and  $T$  is the frequency-dependent *transfer function*, is one of them. It arises from the statistical fluctuation in photon counts, governed by the *Poisson distribution*. Since measuring power at its most fundamental level means counting the rate at which photons strike the detector, statistical fluctuations become very important. It can be clearly seen that photon shot-noise depends inversely on the  $\sqrt{P_{in}}$ , the input laser power. Thus, maximizing the power minimizes the noise. Therefore, it is desirable to make the input laser beam as powerful as possible. We want to minimize the shot-noise in order to achieve a better *signal-to-noise-ratio*, and thus increase our sensitivity.

### 3 PSL Operation

#### 3.1 Gaussian Beams

The transverse profile of the output laser beam takes the shape of Hermite-Gaussian functions, which are the paraxial solutions (eigenmodes) to the scalar wave equation

$$\nabla^2 u + k^2 u = 0, \quad k = \frac{2\pi}{\lambda}. \quad (5)$$

These solutions come in the following form:

$$u = \psi(x, y, z) e^{-ikz}, \quad (6)$$

and trying a solution of this form results in

$$\psi = e^{-i(P + \frac{k}{2q} r^2)}. \quad (7)$$

Here  $P(z)$  is the *complex phase shift*,  $r^2 = x^2 + y^2$ , and  $q(z)$  is the *complex beam parameter*. The  $q$  parameter can be used to completely describe the propagation of a

Gaussian beam. First of all,  $q$  can be propagated in a very straightforward way

$$q_2 = q_1 + z, \quad (8)$$

where  $z$  is the distance between two planar cross-sections ( $xy$  - plane) of the beam. Then,  $q$  is related to two real parameters, *radius of curvature*  $R(z)$  and *beam waist size*  $w(z)$  in the following way:

$$\frac{1}{q} = \frac{1}{R} - i \frac{\lambda}{\pi w^2}. \quad (9)$$

With these relationships, we can completely model the propagation of a Gaussian beam through a system of optical elements (e.g. lenses) using  $q$ . At the waist,  $R \rightarrow \infty$ , and  $q$  becomes purely imaginary, according to

$$q_0 = i \frac{\pi w^2}{\lambda}. \quad (10)$$

Now, complex  $q$  can be propagated through optical elements using simple and elegant formulation of *ray transfer matrices* by thinking of a spherical Gaussian wave as a collection of rays. Because  $R$  follows the simple lens law

$$\frac{1}{R_2} = \frac{1}{R_1} - \frac{1}{f}, \quad f = \text{focal length}, \quad (11)$$

and since  $w$  does not change if we take the limit of a thin lens,  $q$  follows the same relationship:

$$\frac{1}{q_2} = \frac{1}{q_1} - \frac{1}{f}. \quad (12)$$

Thus, if the ABCD matrix is known for a given element (or set of elements),  $q$  can be propagated through it via

$$q_2 = \frac{Aq_1 + B}{Cq_1 + D}, \quad (13)$$

known as the ABCD Law. Then  $w$  and  $R$  can be found from the real and imaginary parts in (9).

### 3.2 Guoy Phase Shift

The exact analytical solution for the lowest order Gaussian beam propagating in free space is [2]

$$u(x, y, z) = \left(\frac{2}{\pi}\right)^{1/2} \frac{\exp(-ikz + i\phi(z))}{w(z)} \exp\left(-\frac{x^2 + y^2}{w^2(z)} - ik\frac{x^2 + y^2}{2R(z)}\right). \quad (14)$$

$$\phi(z) = \tan^{-1}\left(\frac{z\lambda}{\pi w_0^2}\right). \quad (15)$$

The extra  $\phi(z)$  phase shift is due to the transverse profile of the beam, and in general, for higher order Hermite-Gaussian beams it will depend on the mode. Thus, we can deploy the so-called Guoy phase shift in order to filter out all non TEM<sub>00</sub> modes in a resonant cavity by changing the geometry of the end mirrors, choosing the shift in such a way that only TEM<sub>00</sub> will resonate, while other modes will experience destructive interference due to the Guoy effect.

### 3.3 Mode Matching

Mode matching is an important concept in beam propagation. In order to be able to control the beam via servos, the beam must encounter certain devices, such as a Pockels Cell or an Acousto-Optic Modulator (AOM) on its path. The beam must be well placed, so that the waist falls on these devices. This can be achieved by using paired mode matching lenses that effectively change the radius of curvature of the beam. Given two lenses with known focal lengths and the initial position and size of the beam waist, one can find the best positions for the two lenses in order to place the next beam waist as close to the desired destination as possible. In the PSL setup, a number of mode matching lenses is deployed, and keeping them in the right positions is very important.

### 3.4 Mode Mismatch

The output laser beam should be in a circular TEM<sub>00</sub> mode – a simple Gaussian bell shape in both  $x$  and  $y$  directions. It is desirable to keep this mode and this mode only, because the detector design allows only one mode to resonate in its cavities. If everything is done right, only the TEM<sub>00</sub> mode will resonate in the reference cavity. However, if the beam is not perfectly centered on the cavity waist (it could be offset by  $\Delta z$  along the cavity axis, by  $\Delta x$  above the axis, rotated by an angle  $\theta$  with respect to the cavity axis, or differ from the cavity waist size by  $\Delta w$ ), there will be mode mismatch, or unwanted excitation of higher order modes. This takes away power from the main TEM<sub>00</sub> mode and will not couple to the LIGO interferometer optics, and thus should be minimized. If  $V_0$  is the fundamental mode, and  $V_1$  is the first higher mode, the coupling coefficients for waist resizing and misplacement turn out to be [3]

$$\epsilon_1 = \frac{w}{w_0} - 1 \quad \text{and} \quad \epsilon_2 = \frac{\lambda \Delta z}{2\pi w_0^2}. \quad (16)$$

Thus, the goal is to minimize the combined  $\epsilon = \sqrt{\epsilon_1^2 + \epsilon_2^2}$  in

$$\Psi(r) \simeq A(V_0(r) + \epsilon V_1(r)). \quad (17)$$

### 3.5 MOPA Laser

The 126 MOPA, or *Master Oscillator Power Amplifier*, is the Nd<sup>3+</sup>:YAG laser that drives the 40-meter LIGO prototype interferometer at Caltech and the LIGO sites. It is a diode-pumped, narrow-linewidth, single-frequency (1064  $\mu\text{m}$ ) laser with double-pass power amplifier, produced by Lightwave Electronics Inc. The laser produces two distinct output beams, the 10  $W$  main beam, and the 50  $mW$  reference beam that goes to the reference cavity. The emerging beam is in circular TEM<sub>00</sub> mode and is vertically polarized.

Three actuators control the output of MOPA. The PZT attached to the Nd<sup>3+</sup>:YAG crystal does the fast tuning, heating the crystal provides means for slow tuning, and



Figure 3: Hanford LIGO site.

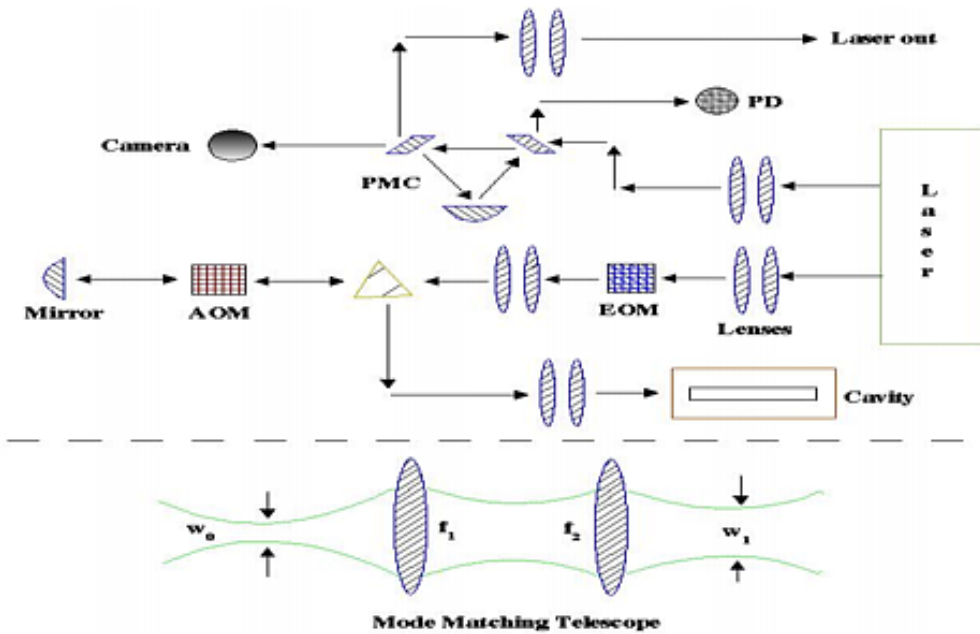


Figure 4: Basic PSL layout.

controlling the AC current in the pump diodes provides additional control.

### 3.6 Frequency Reference Cavity

The frequency reference cavity is the endpoint of the reference beam emerging from the PSL. Unlike the main beam, the reference beam never gets delivered to the interferometer. It is a low power laser beam serving the single purpose of sensing the fluctuations in frequency of the laser in order to stabilize it. When the cavity is locked (i.e. the reference beam is resonating inside of it), the servos keep it in lock by either actuating the PZT attached to the laser crystal (fast), or by heating the crystal itself (slow), thus minimizing fluctuations and drifts in laser output frequency. The reference beam path resembles a miniature version of one of the real interferometer arms with a Fabry-Perot cavity.

### 3.7 Pre-Mode Cleaner

The Pre-Mode Cleaner, or PMC, is a triangular resonant cavity consisting of two partially reflective flat mirrors and one strongly curved mirror at the third vertex. The curved mirror makes the cavity more stable. The PMC's function is to leave only the  $TEM_{00}$  mode in the emerging beam. If any other Hermite-Gaussian modes of higher order are present in the incident beam, they will not resonate in the PMC and will be reflected. Thus, the PMC "cleans" the incident beam, defining its own waist position and radius. Thus, as long as the PMC is properly aligned, and the incident beam is delivered correctly (i.e. mode matching is properly implemented), the emerging beam satisfies the PSL specifications and can be delivered into the interferometer. The difficulty in implementation is achieving a high transmission coefficient for the  $TEM_{00}$  mode. Otherwise, if the PMC is misaligned or the beam is delivered into it incorrectly, the incoming light will not couple to the PMC resonant modes, and too much light will be lost in the cavity.

## 4 Simulating the Beam

In this project, I began by writing a set of Matlab routines to model the propagation of the laser beam on the PSL optical table. I implemented beam propagation using the ABCD law and propagated the *complex beam parameter* through each lens, tracing the width of the beam in both  $x$  and  $y$  throughout its path on the table. The complete result of such calculations is illustrated in the Figures 6 and 7 and in Tables 1, 2, and 3. Each plot produces a graph of  $x$  and  $y$  beam radii along side each other, shows the location of all important elements in the path, and calculates the resulting mode-mismatch coefficient when the beam is delivered into the resonant cavity (reference or PMC). Because of significant differences in layout, two separate sets of routines were implemented for the reference and the main beams.

I also implemented Matlab routines for moving the elements on the table, solving mode-matching problems with two given lenses, and finding the best lens pair for a particular mode-matching problem. Thus, a complete set of tools for simulating and manipulating the PSL table layout now exists. It is relatively easy to find an optimal solution (there are infinitely many if we do not restrict ourselves to a given pair of lenses) to the PSL layout now, provided that the desired locations and radii of beam waists are known.

## 5 Beam Measurements

### 5.1 Transmission

A measurement of the transmitted intensity shows how much light is transmitted through a resonant cavity (reference cavity or the PMC cavity) by observing a peak appearing on the oscilloscope display when the cavity is in resonance. If a photodetector is placed at the end of the beam path, after it has passed through the cavity, and if an oscilloscope



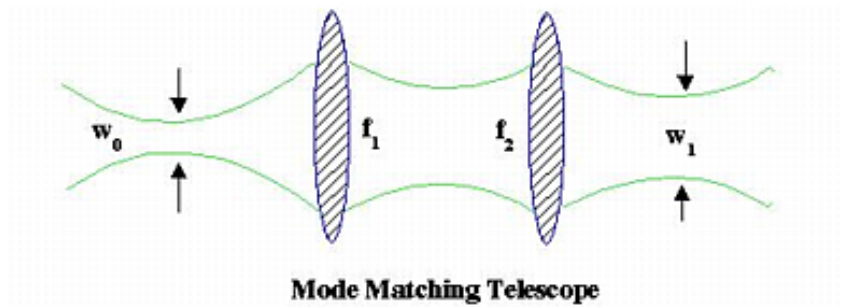


Figure 5: Mode Matching Problem.

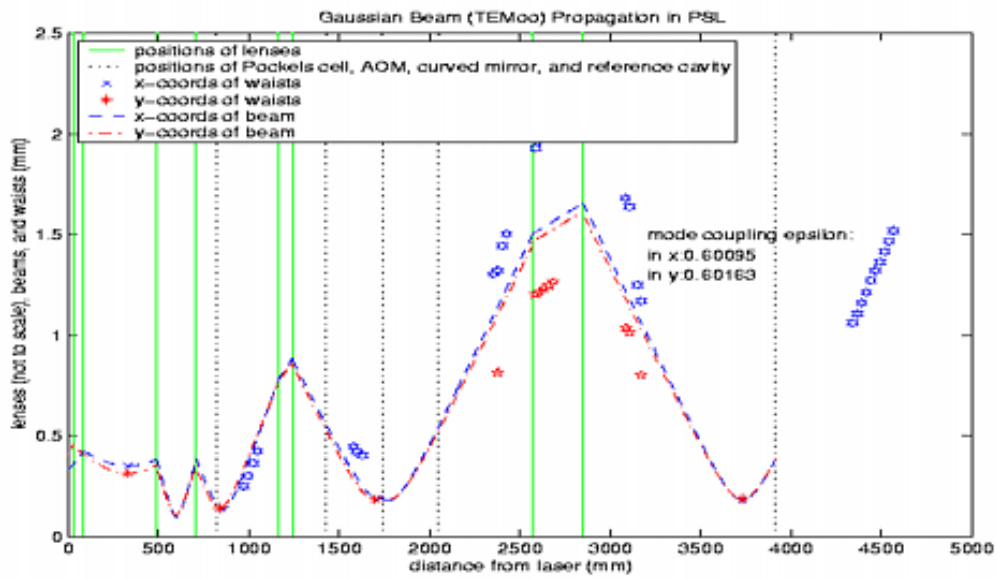


Figure 6: Sample simulation output in Matlab for the reference beam path.

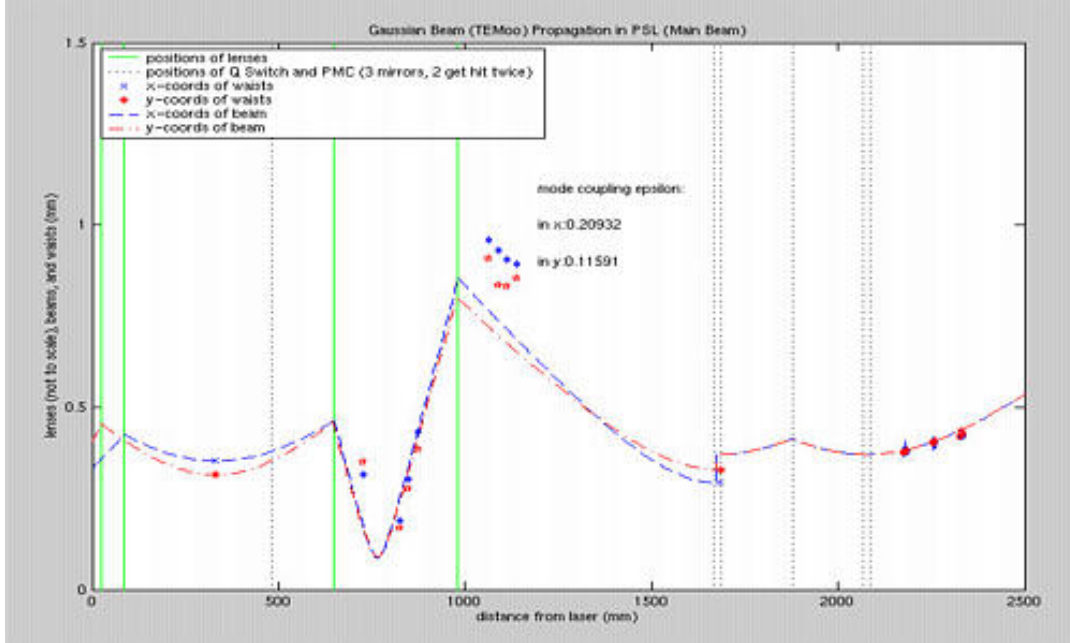


Figure 7: Sample simulation output in Matlab for the main beam path.

Table 1: Lenses and beam parameters in the reference beam path.

Lens	$z_{lens}$ (mm)	$f_{lens}$ (mm)	Waist	$z_x$ (mm)	$z_y$ (mm)	$w_x$ (mm)	$w_y$ (mm)
1 (cylindrical)	25	169.7	1	331.8	328.8	0.353	0.315
2 (cylindrical)	85	250.9	2	853.6	837.3	0.135	0.143
3	490	103.2	3	1725.3	1697.1	0.189	0.185
4	707	68.7	4	3732.3	3729.0	0.182	0.188
5	1160	687.5					
6	1241	286.5					
7	2565	1145.6					
8	2847	687.5					

Table 2: Lenses and beam parameters in the main beam path.

Lens	$z_{lens}$ (mm)	$f_{lens}$ (mm)	Waist	$z_x$ (mm)	$z_y$ (mm)	$w_x$ (mm)	$w_y$ (mm)
1 (cylindrical)	25	169.7	1	331.8	328.8	0.353	0.315
2 (cylindrical)	85	250.9	2	1683.4	1687.7	0.293	0.328
3	648	103.2					
4	981	171.9					

Table 3: Optimal lenses and beam parameters in the reference beam path (to be implemented in the future).

Lens	$z_{lens}$ (mm)	$f_{lens}$ (mm)	Waist	$z_x$ (mm)	$z_y$ (mm)	$w_x$ (mm)	$w_y$ (mm)
1 (cylindrical)	25	169.7	1	328.5	328.8	0.317	0.315
2 (cylindrical)	77	226.7	2	817.0	802.6	0.368	0.369
3	490	458.2	3	1426.0	1420.9	0.140	0.138
4	741	687.5	4	3895.3	3892.4	0.216	0.214
5	1160	229.1					
6	1344	229.1					
7	2565	572.7					
8	3009	802.0					

is in turn connected to the detector, we can observe a peak in intensity occurring on the screen when one of the Hermite-Gaussian modes is resonant in the cavity. Using a CCD camera, one can determine which mode this corresponds to, and try to lock the cavity in the desired TEM<sub>00</sub> mode.

## 5.2 Visibility

This measurement is very similar to the transmitted intensity measurement, except here we look at the light that was reflected from the cavity. If the cavity is in resonance, we should observe a sharp dip in reflected intensity on the oscilloscope display. The deeper the dip, the better the visibility

$$V = 1 - \frac{P_{ref}}{P_{inc}},$$

where  $P_{ref}$  = power reflected, and  $P_{inc}$  = power in the incident beam.

## 5.3 Transverse Profile

Transverse profile tells us how Gaussian the beam is, how circular it is, and exactly how wide it is in  $x$  and  $y$ . These measurements have been made with the *Beam Scan* device so far, but may be conducted with a Spiricon CCD-driven device in the future.

## 5.4 Beam Scan

Beam Scan measurements are of particular interest and importance, because they can give a complete picture of the transverse profile of the laser beam at any accessible point on the table. The device allows us to measure the *intensity cross-section* of the laser beam in the  $xy$ -plane. Beam Scan provides a number of features that are very helpful in learning about the actual beam behavior. These features include:

- calculation of beam width at  $\frac{1}{e^2}$  in intensity ( $I$ ) in both  $x$  and  $y$  – shows how circular the beam is (it should be perfect circle in TEM<sub>00</sub> mode).

Parameter	Value	Mean	Std Dev
13.5% Width A1( $\mu\text{m}$ )	853	866.3	12.4
13.5% Width A2( $\mu\text{m}$ )	857	851.5	12.9
Gaussian Fit A1	0.52	0.656	0.080
Gaussian Fit A2	0.57	0.586	0.133

Figure 8: Sample Beam Scan screen – beam parameters.

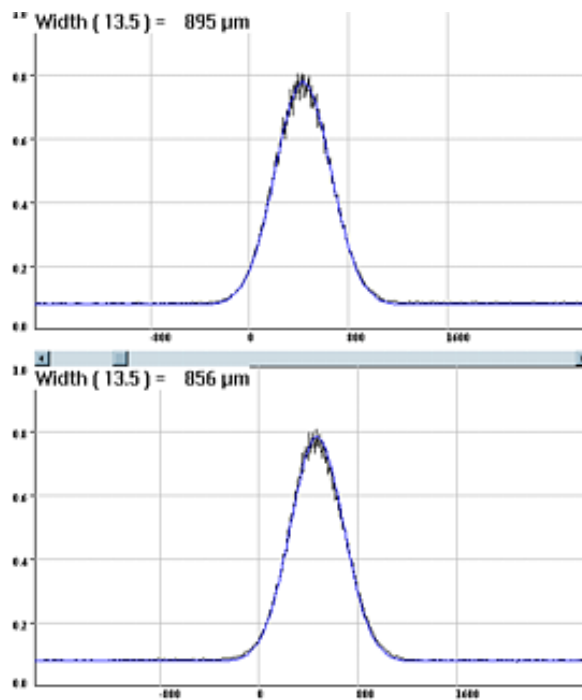


Figure 9: Sample Beam Scan screen – beam plot with Gaussian fit.

- eccentricity of the beam – calculate the ratio of  $I$ 's at two different points along the beam profile curve and compare this to the ratio of  $I$ 's at the same two points on a perfect Gaussian bell-curve fit to the set of points obtained by scanning the beam.
- locating the point maximum Intensity in  $xy$ -plane – if repeated measurements are taken along the beam path, and if the Beam Scan is translated accurately along a line through the optical elements' centers, this will show if the beam drifts away from its path. (This could be difficult to do and, therefore, bears limited value).
- 2-D and 3-D contour drawings of the beam profile – allows to roughly estimate the quality of the beam (i.e. how Gaussian, how circular, how well-centered, how close to TEM<sub>00</sub>), but mostly good for creating eye-pleasing plots.
- multiple samplings – allows to average beam parameters over a series of repeated measurements, providing mean and standard deviation for the set of samples.
- fitting a perfect Gaussian to the measurements and plotting it along with the actual beam data.
- calculating k-factor – describes magnification of the beam by a lens or a system of lenses, unmask any presence of non-fundamental Hermite-Gaussian modes in the beam.

## 6 Results

### 6.1 Optical Table

After I had a complete picture of the simulated beam, I took a number of Beam Scan measurements, so far paying attention to the beam widths only, and plotted the results alongside my simulations. The measurements for the most part agreed pretty well with

my expectations (see the star-plots in Figures 6 and 7), which showed some serious deviations from desired behavior, according to PSL specifications. While in the case of the reference beam this appeared to cause little problem, since the cavity measurements yielded 95% visibility, for the main beam this caused significant problems, as the PMC cavity could not yield visibilities above 5%. After trying to find an optimal set of lenses for delivering the main beam to the PMC cavity waist, I found that the two lenses on the table simply had to be switched. This was implemented, bringing visibility up to 90%.

I have also found the optimal solution to the layout of the reference beam path, working together with LIGO's Michael Smith. If implemented in the future, this layout will ensure that the beam remains circular throughout its path and that it is delivered correctly to the relevant elements (e.g. AOM and EOM) on the table in terms of position and size of the beam waist. See Figure 12 for the final simulation of this refined layout.

## 6.2 Focal Length Measurements

In addition to studying and refining the PSL table layout, I constructed a simple setup that allows one to quickly verify focal lengths of PSL lenses. Since the lenses can be mislabeled or not marked at all, it is sometimes hard to keep track of them on the table, thus increasing the possibility of a layout error. It is, therefore, desirable to have a quick and easy way of determining the focal length of each lens used on the table. My apparatus consists of a HeNe laser, two steering mirrors, a slider consisting of two parallel rulers fixed to the table and a lens mount that can slide freely between them, and a beam stop with a simple bulls-eye type target. The beam is focused on the target, a lens is introduced and moved back and forth along the slider until the focusing spot is found. Since the beam is collimated, the distance from the lens to the target is exactly the focal length we seek. (see Figure 13)

## 6.3 Quad Photodiodes

I have also helped Michael Smith to install two *Quad Photodiodes (QPDs)* in the main path of the beam. These two serve as position and angle monitors. As discussed earlier, the beam can be propagated through its path using the ABCD lens law. If the beam is passed through a single lens, the resulting propagation matrix is

$$\begin{pmatrix} A & B \\ C & D \end{pmatrix} = \begin{pmatrix} 1 - \frac{d_2}{f} & d_1 + d_2 - \frac{d_1 d_2}{f} \\ -\frac{1}{f} & 1 - \frac{d_1}{f} \end{pmatrix}, \quad (18)$$

where  $d_1$  is distance to the lens,  $d_2$  is distance from the lens to the QPD, and  $f$  is the focal length of the lens. From here we see that if we want to decouple position from angle, we can set coefficients  $A$  or  $B$  to zero. Setting  $A$  to zero implies setting  $d_2 = f$ , i.e. placing the QPD in the focal spot of a known lens. This allows us to monitor the angle of the beam exclusively. On the other hand, setting  $B$  to zero leads to

$$f = \frac{d_1 d_2}{d_1 + d_2} \quad \longrightarrow \quad \frac{1}{f} = \frac{1}{d_1} + \frac{1}{d_2}. \quad (19)$$

This is the well known *imaging* situation in Ray Optics, and it provides us with a means of monitoring only the position of the beam.

The two QPDs were installed on the PSL table accordingly and connected to the LIGO *Data Acquisition System (DAQ)*. Using these two QPDs, we can now look for drifts in position and angle of the laser beam over time.

## 6.4 Final Measurements

### 6.4.1 Transmission

Final measurements of transmitted power were made by Dennis Ugolini after the PSL had been locked continuously for over a week. A calorimeter was used to measure the power incident on the PMC and the power emerging from it. The power incident was



$P_{inc} = 2.2mW$  and the power transmitted was  $P_{trans} = 1.4mW$ , yielding a transmission coefficient of  $t = 64\%$ .

#### 6.4.2 Visibility and Beam Scan Profile

Together with Dennis Ugolini, I made the final visibility measurement. The dip in the reflected light's intensity covered 4 out of 7 divisions on the oscilloscope screen connected to the photodiode at the end of the reflected path. Thus, the visibility was  $V = 57\%$  at the end of my project. This was far lower than 80-90% visibilities obtained earlier. The decrease could have been caused by some accidental alteration of the PSL layout during the installation of QPDs. Although this presents a setback for PSL operation, it will most likely be corrected in the nearest future to regain the previously achieved high visibility levels.

The final Beam Scan measurements were taken with the laser in lock (both PMC and reference cavity). The data points obtained for the reference cavity path confirmed earlier measurements. As can be seen in Figure 7, the last set of points obtained for the beam reflected off the reference cavity's front mirror fit very well with the mathematical model's prediction. However, the light reflected off the PMC's front mirror exhibited strange behavior. As can be seen in Figure 7, the model and the measurements differ significantly. This again can be evidence for some accidental change to the main beam setup during installation of the QPDs.

#### 6.4.3 Conclusion

This project has produced simple tools for modeling the propagation of the laser beam on the LIGO 40-meter lab's PSL table. Many measurements taken with the Beam Scan device confirmed the validity of such simulations. Additional tools were implemented that allow one to solve various mode-matching problems often found in construction of a laser setup. As the result, a rather complete set of tools for working with the PSL layout

has been developed and tested. Simulations have produced solutions that have already resulted in improved performance in the main beam and, if implemented in the future, will correct the mode-matching problems that result in loss of power in the reference path.

## 7 Acknowledgments

People and organizations that have provided help and guidance in this project include my mentor Alan Weinstein, LIGO postdoc Dennis Ugolini, LIGO engineers Mike Smith, Ben Abbot, and Stephen Vass, Caltech professor Kenneth Libbrecht and many other people involved in the LIGO project, and the Caltech SURF summer program.

## References

- [1] Saulson, Peter. *Fundamentals of Interferometric Gravitational Wave Detectors*. World Scientific Publishing Co. 1994.
- [2] Siegman, Anthony. *Lasers*. University Science Books. 1986.
- [3] Anderson, Dana. "Alignment of Resonant Optical Cavities." *Applied Optics*, Vol. 23, No. 17. September 1, 1984.
- [4] Kogelnik and Li. "Laser Beams and Resonators." *Applied Optics*, Vol. 5, No. 10. October 1966.
- [5] Abbot R., King P. "Pre-stabilized Laser (PSL) Final Design." LIGO Technical Note. March 8, 1999.

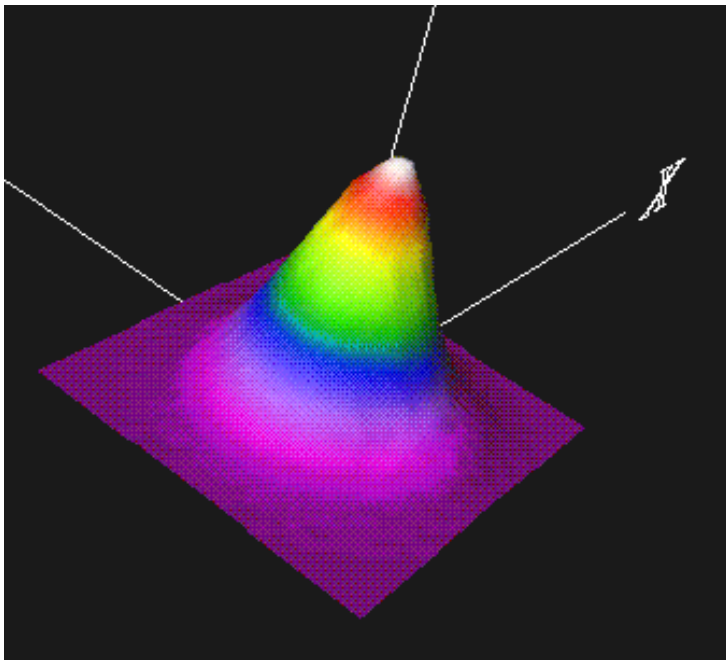


Figure 10: Sample Beam Scan screen – 3D beam plot.

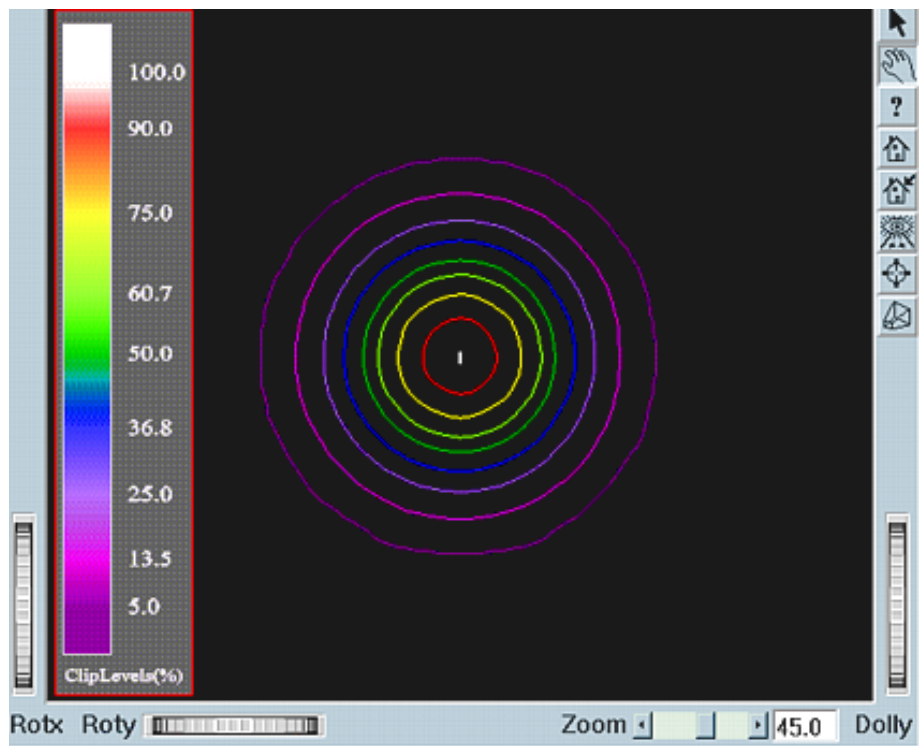


Figure 11: Sample Beam Scan screen – 2D contour beam plot.

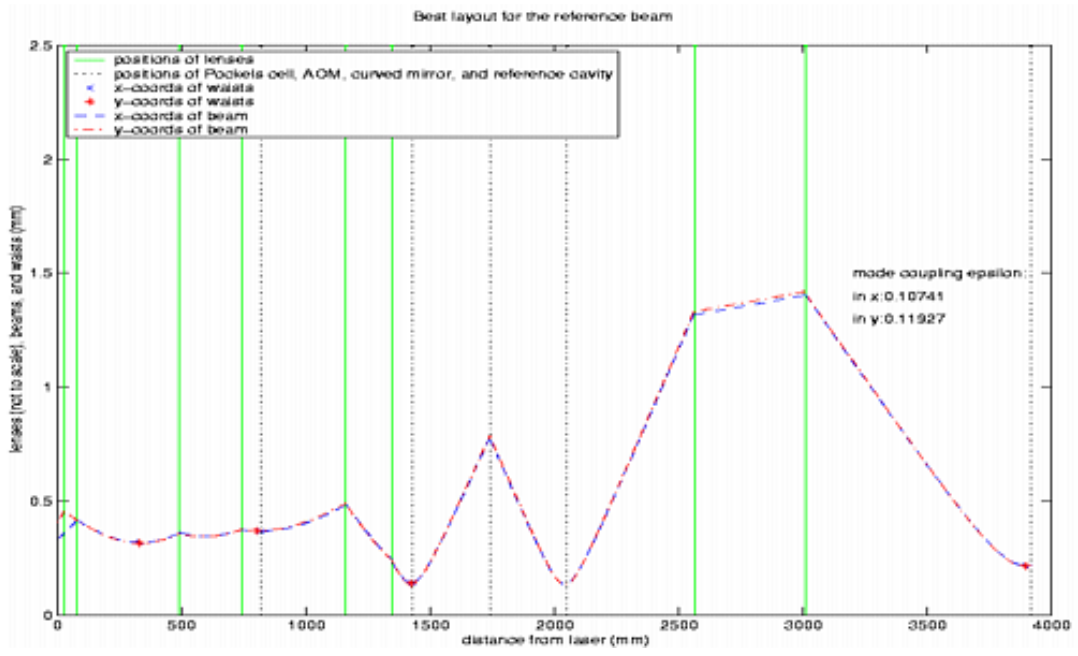


Figure 12: Matlab simulation of the optimal layout for the reference beam path.

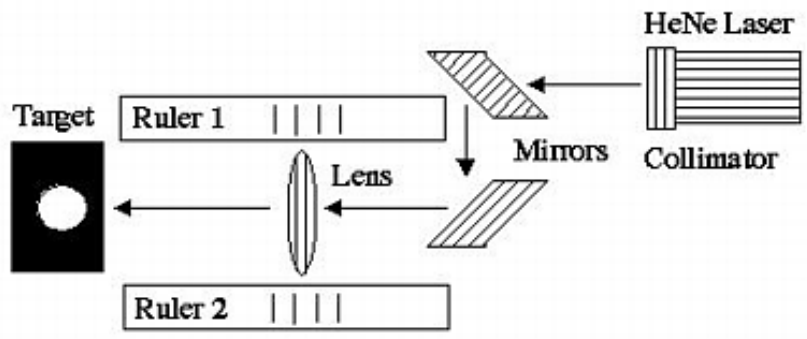


Figure 13: Setup for measuring focal lengths of lenses used in PSL layout.

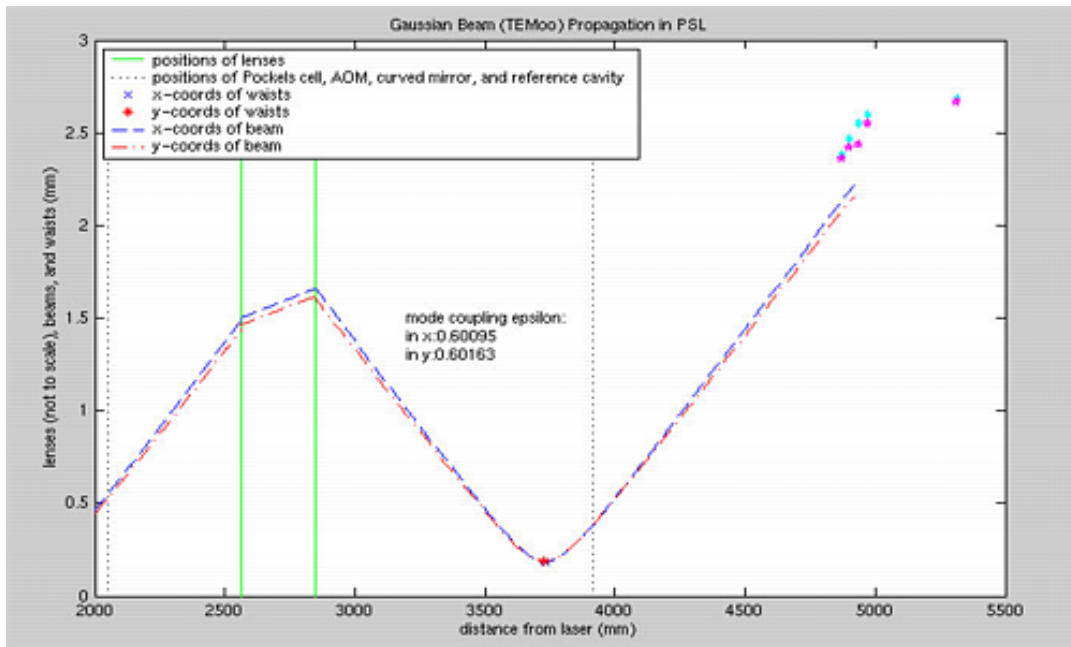


Figure 14: Final beam scan measurements in the reference beam path confirm previous data (data points shown as pentagams and hexagams).

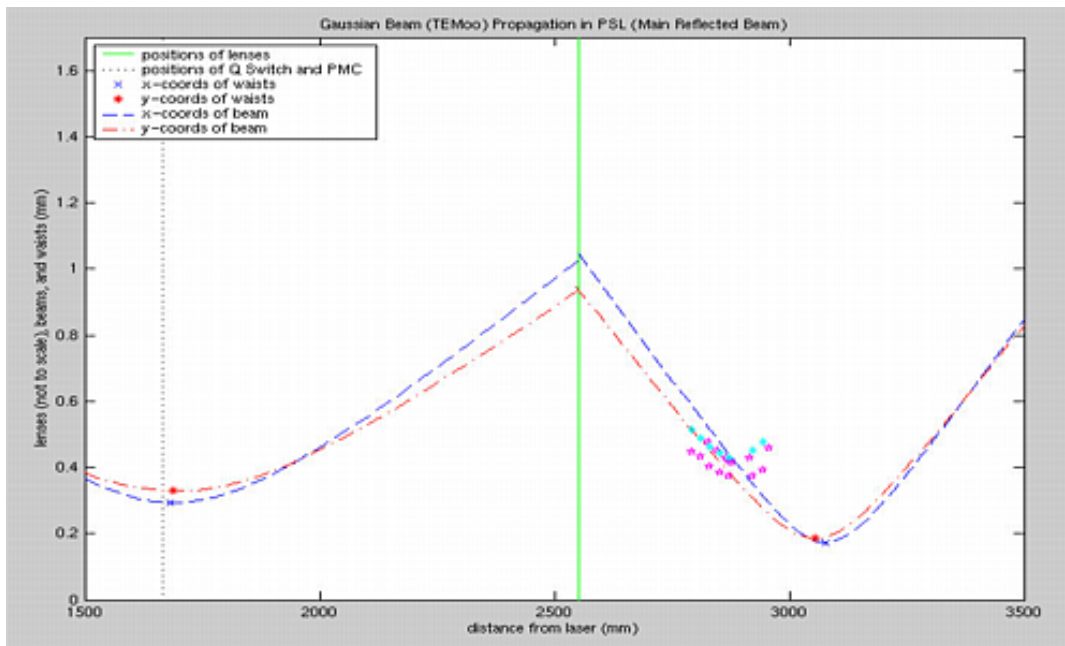


Figure 15: Final beam scan measurements in the main beam path show that something has probably changed in the PSL layout since the initial set of measurements was obtained.